ELSEVIER

Journal of Chromatography A, 707 (1995) 105–116

JOURNAL OF CHROMATOGRAPHY A

Combined continuous and preparative chromatographic separation

Kyung Ho Row

Department of Chemical Engineering, INHA University, 253 Yonghyun-Dong, Nam-Ku, Inchon, South Korea

Abstract

A combined continuous and preparative gas–liquid chromatographic system was considered for the separation of the close-boiling components diethyl ether and dichloromethane. The characteristics of the combined continuous and preparative gas–liquid chromatographic system were investigated in terms of the experimental operating conditions. It was experimentally confirmed that the additional column length and the desorbent velocity were the most important factors to ensure the continuous separation of the feed mixture. The theoretical concentration profiles were calculated by a mathematical model with the assumptions of uniform film thickness and linear partition equilibrium. Although small deviations between the calculated profiles and the experimental data were observed, the model might be used as a predictive tool for determining the optimum operating conditions for the combined continuous and preparative chromatographic system.

1. Introduction

Gas chromatography is a separation method based on differences in the partition coefficients of substances distributed between a stationary liquid phase (SLP) and a mobile phase. Since the introduction of gas chromatography [1], over the past 30 years much efforts have been made to increase the throughput capabilities. Until now, attempts have been made to scale up lab-sized chromatographic units to treat larger quantities of substances and to bring these systems to preparative or process-scale operation [2,3].

Generally the chromatographic processes fall into two main categories, i.e. batch and continuous. Batch-type processes were first developed in 1953 and commercial units are now available [4]. Continuous systems were introduced soon after 1955 and in recent years work on this type of system has mainly concentrated on increasing their throughputs [1,2,5]. Among the systems to meet the conditions of high troughput, the UOP (Universal Oil Products) process is widely acknowledged as a useful system [6]. As an improved preparative chromatography, Wankat [7] and Ha et al. [8,9] developed moving feed point chromatography. This was later combined with moving product withdrawal chromatography, and moving port chromatography was suggested [10]. Wankat properly used a local equilibrium model to analyze the characteristics of the system. Two mathematical models of the moving bed adsorber, an intermittent moving bed and a continuous moving bed type, were presented by Hashimoto et al. for calculating the concentration profiles of glucose and fructose [11,12].

Such mixtures as various hydrocarbons, dextran, and saccharoids were separated using series of semicontinuous counter-current refiners (SCCR) [13–15] and a mathematical model

0021-9673/95/$09.50 © 1995 Elsevier Science B.V. All rights reserved
SSDI 0021-9673(95)00529-3

based on the theoretical plate concept was used to simulate the performance of the unit [16]. For the SCCR unit and the UOP process, Ching and Ruthven have proposed a theoretical model for simulated counter-current operation as an equivalent counter-current cascade of theoretical equilibrium stages under steady-state condition and obtained the analytical concentration profile [17,18].

In this paper, a continuous separation method is utilized in which binary feed mixtures are separated by the combined continuous and preparative chromatographic system in two steps (partition and desorption). Although the system is equipped with segmented columns and the less-absorbed or less-adsorbed component can be obtained in pure form in the partition or adsorption section as in other continuous systems, the remaining components in the columns can also be separated in the desorption section by changing the operating conditions such as column length and desorbent velocity. Mathematical models for this combined continuous and preparative chromatography have been developed and used to investigate the usefulness of the system and the effects of operating conditions on the resolution of the two close-boiling components by prediction of their concentration profiles. We also compared the experimental data with the calculated values to confirm the mathematical models.

2. Operational principles of the system [19]

In the present system, binary feed mixtures of diethyl ether (DEE) and dichloromethane (DCM), are separated continuously with the combined continuous and preparative chromatography taking place in two sections, i.e. the partition and desorption sections.

When a feed mixture is injected into a single column, the less-absorbed component (DEE) is eluted initially by the solubility difference between the feed mixture and the SLP. After a while, as the more-absorbed component (DCM) also begins to be eluted, the components are eluted from the column in a composition which is

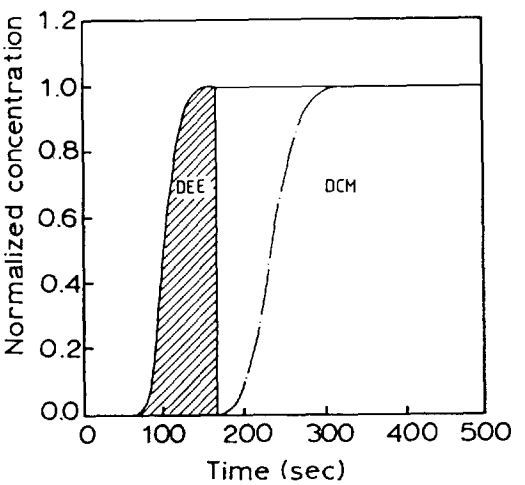

Fig. 1. Theoretical concentration profile in case of step input.

the same as that of the feed mixture. As shown in Fig. 1, the less-absorbed component is eluted as a pure product (the shaded portion in the figure) until the second component starts to elute, so during that time pure DEE can be collected. Here, we define the normalized concentration used in the system as the ratio of the concentration of a component in the mobile phase to the concentration of that component at the inlet of the column, c/c_0.

Fig. 2 shows the arrangement of the columns and solenoid valves. During operation of this system, two streams, i.e. the carrier gas with feed and the desorbent, enter the system, and two product streams leave the system through the partition section and the desorption section.

The principles of the combined continuous and preparative chromatographic system are based on switching the configuration of the columns. The less-absorbed component can be obtained in pure form before the elution of the more-absorbed component in the partition section starts. During that time, in the desorption section, the less-absorbed component remains in the column while the more-absorbed component can be separated by adjusting the additional column length and the desorbent velocity. If the above two steps can be simultaneously completed within a certain time (switching time), the binary feed

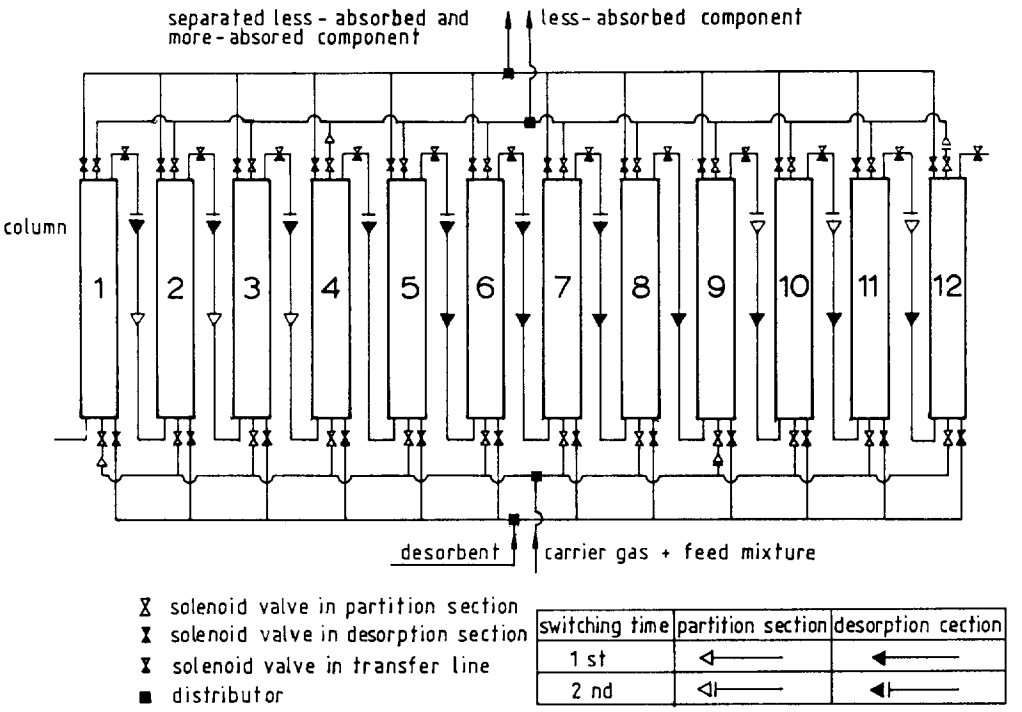

Fig. 2. Configuration of columns and solenoid valves.

mixture can be separated continuously. The switching time depends on the characteristic combination of the stationary liquid and the feed mixture. In the desorption section, the remaining components should be separated within the switching time by changing the operating conditions.

For example, the partition section consists of four columns (e.g. columns 1–4) and the desorption section of eight columns (columns 5–12). During the first switching time, the feed mixture is continuously injected into the inlet of column 1, and the less-absorbed component is obtained in pure form at the outlet of column 4. Just before the elution of the more-absorbed component, within the second switching time, the feed mixture is injected into the inlet of column 9, which is the starting column of a new partition section (columns 9–12). At the same time, in the desorption section (columns 1–8), the desorbent is injected into the inlet of column 1, and at the outlet of column 8, the remaining less-absorbed component and the more-absorbed components are obtained separately within the switching time.

The segmented columns can be configured and switched by a microprocessor according to the characteristics of feed mixture. The system is a binary separation process, but by the careful selection of the SLP and the operating conditions it can be extended to various feed mixtures.

3. Mathematical models

The distribution of the stationary liquid phase on the solid support appears to be very complex because of irregularities in pore size and shape. The assumptions for establishing the governing equations of the processes are a uniformly distributed stationary liquid phase on the surface of the inert solid particles, a linear partition isotherm, negligible sorption and pressure drop effects, and a spherical shape of the solid par-

ticles [20,21]. As the concept of the uniform film thickness simplifies the phenomena of porous particles coated with the stationary liquid phase, transient material balances for a component are

$$\frac{\partial c}{\partial t} + u\frac{\partial c}{\partial z} = \frac{E\partial^2 c}{\epsilon \partial z^2} - \frac{3}{r_p}\frac{1-\epsilon}{\epsilon} D_e \frac{\partial q}{\partial r} t_{r=r_p} \quad (1)$$

for the mobile phase,

$$\epsilon_p \frac{\partial q}{\partial t} = D_e \frac{1}{r^2}\frac{\partial}{\partial r}\left(r^2 \frac{\partial q}{\partial r}\right) - A_p k_g \left(q - \frac{n|_{x=\delta}}{K}\right) \quad (2)$$

for the intraparticle phase, and

$$\frac{\partial n}{\partial t} = D_l \frac{\partial^2 n}{\partial x^2} \quad (3)$$

for the SLP

The initial and boundary conditions are:

$$c = q = n = 0 \qquad (\text{for } t = 0,\ z > 0) \quad (4)$$

$$c = c_0(t) \qquad (\text{for } t > 0,\ z = 0) \quad (5)$$

$$c = \text{finite} \qquad (\text{for } t > 0,\ z \to \infty) \quad (6)$$

$$\frac{\partial q}{\partial r} = 0 \qquad (\text{for } t > 0,\ r = 0) \quad (7)$$

$$\frac{\partial n}{\partial x} = 0 \qquad (\text{for } t > 0,\ x = 0) \quad (8)$$

$$D_e \frac{\partial q}{\partial r} = k_f(c - q) \qquad (\text{for } t > 0,\ r = r_p) \quad (9)$$

$$D_l \frac{\partial n}{\partial x} = k_g\left(q - \frac{n}{K}\right) \qquad (\text{for } t > 0,\ x = \delta) \quad (10)$$

It is assumed that the partition effect is dominant to the adsorption effect with a linear equilibrium isotherm. In terms of a given axial distance, z, the solution of Eqs. 1–10 in the Laplace domain is

$$C(s) = C_0(s)\exp\left(\frac{z}{2}\left[\frac{u_0}{E} - \left\{\left(\frac{u_0}{E}\right)^2 + 4\lambda\right\}^{1/2}\right]\right) \quad (11)$$

where

$$\lambda = \frac{\epsilon}{E}\left(s + \frac{3(1-\epsilon)}{r_p \epsilon} k_f \left\{1 - \frac{\sinh(\lambda_2 r_p)}{r_p}\lambda_1\right\}\right) \quad (12)$$

$$\lambda_1 = \frac{r_p k_f}{D_e \lambda_2 \cosh(\lambda_2 r_p) + \left(k_f - \frac{D_e}{r_p}\right)\sinh(\lambda_2 r_p)} \quad (13)$$

$$\lambda_2 = \left(\frac{1}{D_e}\left[\{\epsilon_p s + A_p k_g\} - \frac{A_p k_g^2 \cosh\lambda_3}{D_e K\sqrt{\frac{s}{D_l}}\lambda_3 + D_e k_g \cosh\lambda_3}\right]\right)^{1/2} \quad (14)$$

$$\lambda_3 = \delta\sqrt{\frac{s}{D_l}} \quad (15)$$

The usual method of operating fixed beds for preparative scale is to use a large input pulse of feed onto the column followed by a longer period of flow of carrier gas. In case of pulse input, $C_0(s)$ has the following form:

$$C_0(s) = \frac{1 - e^{-st_0}}{s} \quad (16)$$

where t_0 is the time of feed injection. Then Eq. 11 becomes at the bed exit, $z = L$,

$$C(s) = \frac{1 - e^{-st_0}}{s} \times \exp\left(\frac{L}{2}\left\{\frac{u_0}{E} - \left[\left(\frac{u_0}{E}\right)^2 + 4\lambda\right]^{1/2}\right\}\right) \quad (17)$$

Eq. 17 can be used to predict the concentration profile of a feed component in the partition section. It is assumed that in the desorption section the components are partitioned initially with the inlet concentration of the feed, c_0. The governing equations are the same as in the partition section. However, some of the initial and boundary conditions are different from those of the partition section. The initial condition and the boundary condition in the desorption section are changed as follows:

$$c = q = c_0 \quad (\text{for } t = 0, z > 0) \quad (18)$$

$$n = Kc_0 \quad (\text{for } t = 0, z > 0) \quad (19)$$

$$c = 0 \quad (\text{for } t > 0, z = 0) \quad (20)$$

Under these conditions, the solution in the

Laplace domain is at a given length z in the desorption section,

$$C(s) = \gamma\left(\exp\left\{\frac{z}{2}\left(\frac{u_0}{E} - \left[\left(\frac{u_0}{E}\right)^2 + 4\gamma_1\right]^{1/2}\right)\right\} - 1\right) \quad (21)$$

where

$$\gamma = \left(-\frac{\epsilon_p c_0}{E} + \frac{3(1-\epsilon_p)}{r_p E} k_f \left\{\frac{\gamma_2 \sinh(\sqrt{\gamma_4} r_p)}{r_p} + \frac{\gamma_5}{\gamma_4}\right\}\right)/\gamma_1 \quad (22)$$

$$\gamma_1 = -\frac{\epsilon s}{E} + \frac{3(1-\epsilon)}{r_p E} k_f \left\{1 - \frac{\gamma_3 \sinh(\sqrt{\gamma_4} r_p)}{r_p}\right\} \quad (23)$$

$$\gamma_2 = -\gamma_5 k_f/\gamma_4 (D_e\{\sqrt{\gamma_4} r_p \cosh(\sqrt{\gamma_4} r_p) - \sinh(\sqrt{\gamma_4} r_p)\}/r_p^2 + k_f \sinh(\sqrt{\gamma_4} r_p)/r_p) \quad (24)$$

$$\gamma_3 = \frac{-\gamma_4}{\gamma_5 \gamma_2} \quad (25)$$

$$\gamma_4 = \frac{1}{D_e}(\epsilon_p s + A_p k_g) - \frac{A_p k_g^2 \cosh\left(\sqrt{\frac{s}{D_1}}\delta\right)}{D_e K\{\sqrt{D_1 s}\,\mathrm{sing}\left(\sqrt{\frac{s}{D_1}}\delta\right) + k_g \cosh\left(\sqrt{\frac{s}{D_1}}\delta\right)/K\}} \quad (26)$$

$$\gamma_5 = \frac{A_p k_g}{D_e K}\left\{\frac{Kc_0}{s} - \frac{\frac{k_g c_0}{s}\cosh\left(\sqrt{\frac{s}{D_1}}\delta\right)}{\sqrt{D_1 s}\sinh\left(\sqrt{\frac{s}{D_1}}\delta\right) + k_g \cosh\left(\sqrt{\frac{s}{D_1}}\delta\right)/K}\right\} + \frac{c_0}{D_e} \quad (27)$$

Eq. 21 is used for predicting the concentration profiles in the desorption section, and it is also used as an input function for the inlet of additional columns of the desorption section. That is,

$$C_0(s) = \gamma\left(\exp\left\{\frac{L}{2}\left(\frac{u_0}{E} - \left[\left(\frac{u_0}{E}\right)^2 + 4\gamma_1\right)^{1/2}\right]\right\} - 1\right) \quad (28)$$

The governing equations, initial conditions and other boundary conditions are the same as those in the partition section. Therefore, the solution of the desorption section of the column length, L, with the additional column length (L') in the s-domain is

$$C(s) = \gamma\left(\exp\left\{\frac{L}{2}\left(\frac{u_0}{E} - \left[\left(\frac{u_0}{E}\right)^2 + 4\gamma_1\right]^{1/2}\right)\right\} - 1\right) \times \exp\left(\frac{L'}{2}\left\{\frac{u_0}{E}\left[\left(\frac{u_0}{E}\right)^2 + 4\lambda\right]^{1/2}\right\}\right) \quad (29)$$

The resulting Laplace transformed equations (Eqs. 17, 21, and 29) should be converted into the real time domain. For an approximation technique, the equations are inverted numerically with the curve fitting procedure suggested by Dang and Gibilaro [22]. In the numerical inversion, the infinite upper integration limit is taken as the corresponding value of the frequency to the amplitude ratio of the Laplace transformed equations of 0.001, and it takes just about 15 s using HP Vectra (Model 486/66VL) to transform the equations into the real time domain. The kinetic constants and other parameters in the mathematical models are listed in Table 1 [20]. The % liquid loading in the table is defined by the percentage ratio of the weight of stationary liquid phase to that of uncoated solid packings.

4. Experimental

Diethyl ether and dichloromethane were used as feed mixture, and their boiling points are 34.5°C and 40.0°C, respectively. The partition coefficients of DEE and DCM were evaluated on an analytical chromatographic column over wider temperature ranges [23]. Nitrogen was used as carrier gas and desorbent.

Twelve columns were arranged in a circular form. The columns were made of stainless steel, 1 cm I.D., 30 cm height, with a packed height of 25 cm. At both ends of the columns, glass wool was used to keep the solid particles in place. The columns were packed with Chromosorb A (Alltech Associates) which has a sufficient capacity to load the stationary phase and the surface of which is not highly adsorptive, so it is mainly used for preparative-scale separation [24]. Chromosorb A of three different particle sizes (60/80,

Table 1
The kinetic constants and other parameters used in the simulations

$k_f = (D_M)/(2r_p)(2 + 1.45Re^{0.50}Sc^{0.33})$
$k_g = 12.5(D_M(1 - \epsilon_p))/(r_p\epsilon_p)$

Mesh size	60/80			45/60			20/30		
r_p (cm)	0.00996			0.01360			0.03140		
% Liquid loading	25	20	15	25	20	15	25	20	15
ϵ_p	0.62	0.66	0.69	0.62	0.66	0.69	0.50	0.54	0.57
% Liquid loading	25			20			15		
δ (μm)	0.1270			0.0955			0.0650		

Temperature	DEE		DCM	
°C	D_l 10^{-6} cm^2/s	K –	D_l 10^{-6} cm^2/s	K –
25	0.471	184.2	0.595	437.1
35	0.650	126.3	0.901	297.1
45	1.090	88.7	1.275	206.8
D_e ($\times 10^{-3}$ cm^2/s)	1.00		2.00	
ϵ	0.41			
A_p (cm^2/cm^3)	1300000.0			

45/60, and 20/30 mesh) was commercially available. A rotavapor (Brinkmann Co.) was used to coat dinonylphthalate on the particles, and the percentage liquid loading was set at 20% in the experiments with all particle sizes. Each column has four openings, two for entering streams and two for withdrawing streams, and it was covered with ceramic insulation to keep the column temperature constant.

A schematic diagram of the main chromatographic system is shown in Fig. 3 [19,25]. Five solenoid valves (CKD, AB 31-01-4) were arranged around a column. The twelve columns, sixty solenoid valves, and four distributors were fixed to a support and the complete set-up was enclosed in a steel cover to maintain a desired temperature in the system. The four distributors, two for entering streams and two for withdrawing streams, were installed. Each distributor was of a cylindrical type whose upper side had one central bore, and the side of the distributor had twelve screwed openings. The entering stream passed through the central bore and went into one of the openings in the distributor, and then it entered the inlet of the column through the solenoid valve connected with the opening. Conversely, the withdrawing stream through the solenoid valve from the outlet of the column went through one of the openings and the central bore in the distributor, and was finally sent to the analyzer.

The inlet feed mixtures and the two outlet streams from the main system were analyzed by a conventional gas chromatograph (Gow Mac 550P thermal conductivity detector) with a syringe (Hamilton Co.) and a ten-port multi-functional sampling valve (Valco Instruments Co.), respectively. Pressure gauges were set at the

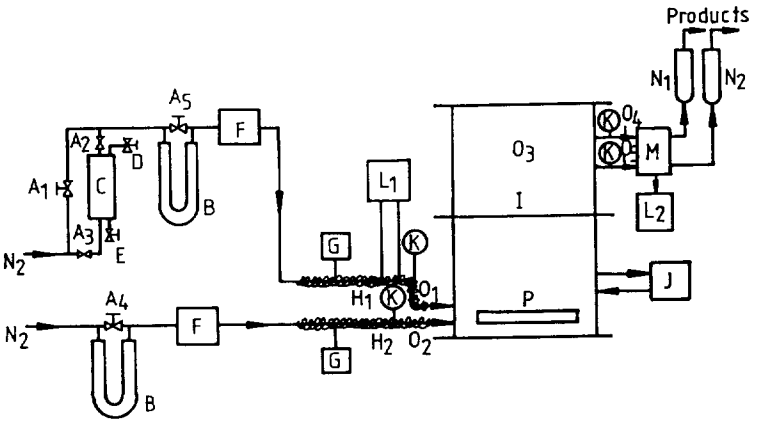

Fig. 3. Schematic diagram of the main chromatographic unit. (A_1,A_4,A_5) Microneedle valves, (A_2,A_3) solenoid valves, (B) manometers for adjustment of flow-rates, (C) feed reservoir, (D) inlet of feed, (E) outlet of feed, (F) preheaters for carrier gas and desorbent, (G) temperature controller, (H_1,H_2) heating wires, (I) main chromatographic system, (J) programmable controller, (K) pressure gauges, (L_1,L_2) gas chromatographs, (M) multifunctional sampling valves, (N_1,N_2) bubble flow meters for carrier gas and desorbent, (O_1–O_5) thermocouples, (P) electric heater.

inlet and outlet of the main system, so the pressure drops of the two sections were recorded. The dead volume of the system was determined from the measurement of the retention time of a helium sample.

The sixty solenoid valves in the main chromatographic system were controlled by a programmable controller. Flow paths of the partition and desorption sections were initially set by the controller, and then they were automatically and consecutively turned to the next step after a switching time.

5. Results and discussion

In a gas chromatographic column, the gas flows through the narrow interstices between the solid support particles packed in the column. The local changes in the viscosity and flow velocity of the gaseous mixture result in the pressure gradient along the column [26]. The smaller the particles the higher the pressure drop (Fig. 4). The velocity gradient will be changed by pressure changes in the column. The average velocity, i.e. the abscissa in Fig. 4, u_{ave}, is the velocity corrected by the compressibility factor as suggested by James and Martin [1]. A pressure drop of 30–90 cmHg was observed in the present experimental set-up. The gas velocity will be more uniform at a low inlet-to-outlet pressure ratio. Therefore, it is desirable to use a rather larger particle size and low flow-rates of the carrier gas or the desorbent in order to separate the feed efficiently.

The total elution volumes of the DEE and DCM mixture are plotted versus the feed concentration and the column temperature in Fig. 5.

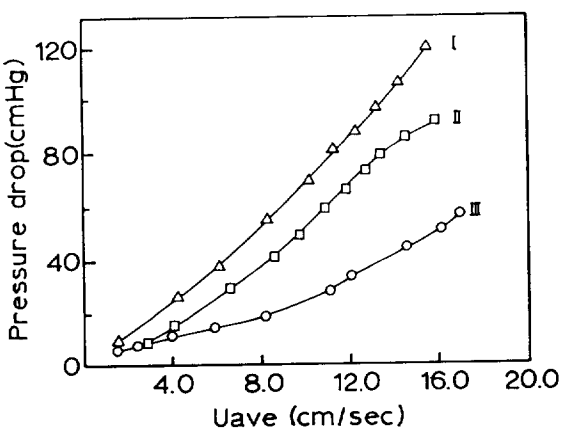

Fig. 4. Effect of particle size on pressure drop; (I) 60/80 mesh, L = 100 cm, (II) 20/30 mesh, L = 200 cm, (III) 20/30 mesh, L = 100 cm.

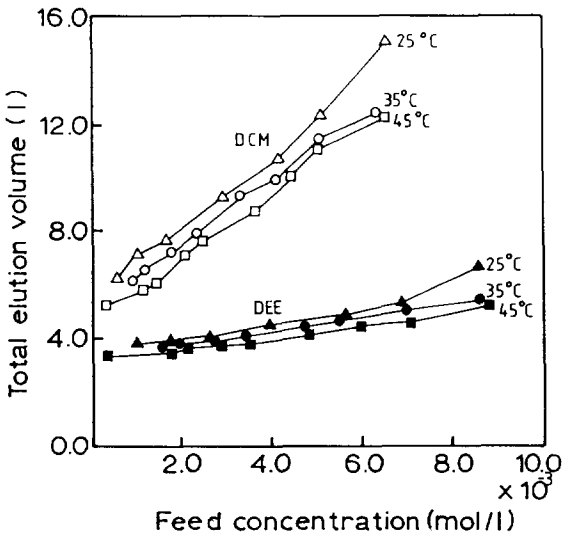

Fig. 5. Effect of feed concentration on total elution volume with column temperatures. (20/30 mesh. $u_{ave} = 9.53$ cm/s, $L = 100$ cm, switching time, 300 s).

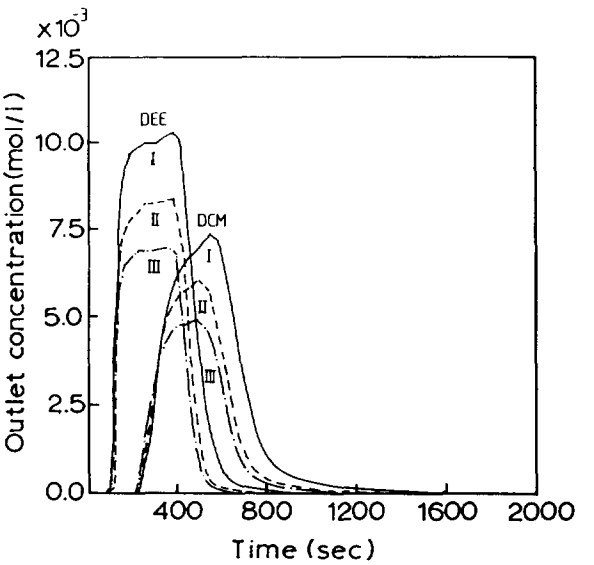

Fig. 6. Effect of feed concentration on elution profile. (I) $c_{0,DEE} = 10.0 \cdot 10^{-3}$ mol/l, (II) $8.3 \cdot 10^{-3}$ mol/l, (III) $6.8 \cdot 10^{-3}$ mol/l; (I) $c_{0,DCM} = 7.3 \cdot 10^{-3}$ mol/l, (II) $6.3 \cdot 10^{-3}$ mol/l, (III) $4.9 \cdot 10^{-3}$ mol/l; 20/30 mesh, 25°C, $u_{ave} = 9.53$ cm/s, $L = 100$ cm, switching time, 300 s.

The total elution volume is the quantity of gas that can elute the components completely from the length of the column. The slope of each component can also be seen in this figure. Although the slope of the elution profile for DEE is low and that for DCM is high, the bandwidth of both components was observed to be wider with increasing feed concentration and decreasing column temperature which resulted from the limited vaporization capacity when feed mixtures with a higher concentration were injected (see Fig. 6). Here, c_0 indicates the inlet concentration of the feed.

The calculated curves in the following figures are the numerical inversion of Eqs. 17, 21, and 29, for the partition section, the desorption section, and the desorption section with additional column length, respectively. The experimental concentration profile for DEE is compared to the calculated values in the partition section (Fig. 7). DCM was not eluted in the partition section, and the agreement between the two profiles was good. The performance of the system in the partition section did not vary greatly with respect to particle size, because the

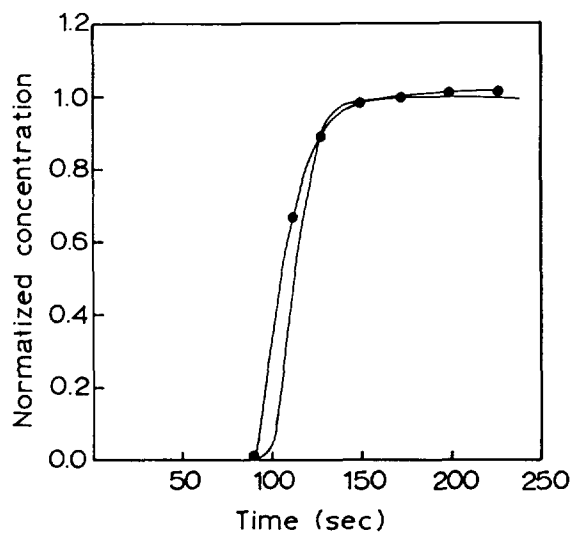

Fig. 7. Comparison of experimental data (●) with calculated values (solid line) for DEE. ($c_{0,DEE} = 0.98 \cdot 10^{-3}$ mol/l, $c_{0,DCM} = 0.91 \cdot 10^{-3}$ mol/l, 45/60 mesh, 35°C, $u_{ave} = 8.80$ cm/s, $L = 100$ cm, switching time, 240 s).

Table 2
Switching times (s) with operating conditions

Temp. (°C)	20/30 mesh		45/60 mesh		60/80 mesh	
L(cm)	100	150	100	150	100	150
25	270	480	300	480	300	480
35	240	360	240	360	240	360
45	180	270	180	300	180	300

switching time was almost constant for the particle sizes used (see Table 2).

Fig. 8 shows the concentration profiles of DEE and DCM in the desorption section. In the model equations (Eqs. 18–20), the initial concentrations were assumed to be proportional to the inlet concentrations of the feed, c_0. This assumption seems to be valid for the less-absorbed component (DEE), but does not seem to hold exactly for the more-absorbed component (DCM). This means that in the partition section, which is to become the desorption section after a switching time, DCM is not uniformly distributed and more likely maldistributed around the inlet of the column, because its partition coefficient is large.

The two components were not fully resolved in the desorption section as shown in Fig. 8. If the desorption section is used exclusively without an additional column, the more-absorbed component can be obtained in pure form after the unseparated mixture is recycled in a batch-type process. Continuous operation, however, can be achieved by connecting the additional columns to the end of the desorption section. As shown in Fig. 9, the resolution between the two components was improved by an additional column

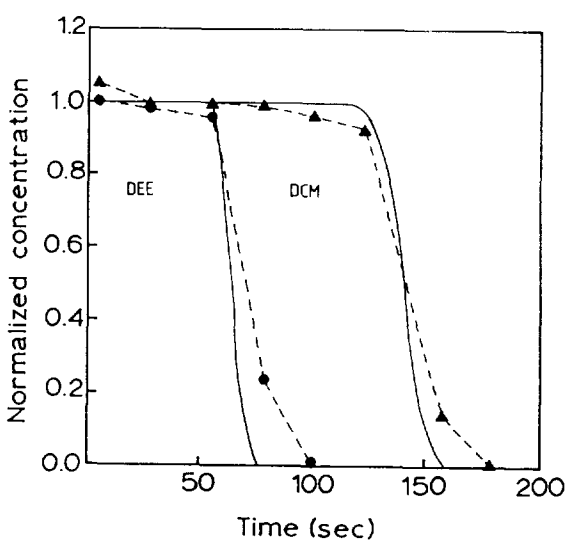

Fig. 8. Comparison of experimental data of DEE (●) and DCM (▲) with calculated values (solid line). ($c_{0,\mathrm{DEE}} = 0.94 \cdot 10^{-3}$ mol/l, $c_{0,\mathrm{DCM}} = 0.78 \cdot 10^{-3}$ mol/l, 45/60 mesh, 45°C, $u_{ave} = 11.30$ cm/s, $L = 100$ cm, switching time 180 s).

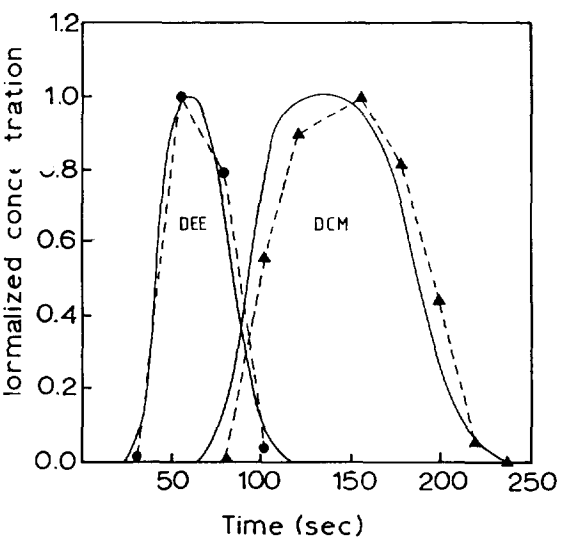

Fig. 9. Comparison of experimental data of DEE (●) and DCM (▲) with calculated values (solid line). ($c_{0,\mathrm{DEE}} = 0.61 \cdot 10^{-3}$ mol/l, $c_{0,\mathrm{DCM}} = 0.57 \cdot 10^{-3}$ mol/l, 20/30 mesh, 35°C, $u_{ave} = 19.90$ cm/s, $L = 100$ cm, $L' = 100$ cm, switching time 240 s).

length of 100 cm. The small differences in the trailing edge of the concentration profile of DEE and in the leading edge of the DCM profile may be partly caused by the assumption of a linear partition equilibrium. With adjustment of only the desorbent velocity, the components remaining in the desorption section with the additional column length can be controlled within the switching time of 240 s.

Flow-rates between 5 and 10 cm^3/h yielded pure DEE and almost completely separated DEE and DCM with column lengths of 100 cm for the partition and the desorption section, 20/30 mesh particle size, 35°C column temperature, and an additional column length of 100 cm [19].

The pressure drop by the smaller particle size and the longer column length caused variation in the gas velocity, and the higher feed concentrations along the length of the column were necessarily accompanied by changes in the velocities. In the present system, the assumption that the velocity of the carrier or the desorbent remained constant throughout the column was compensated by the average gas velocity. Although small differences between the calculated concentration profiles and the experimental data were observed, the uniform thickness model may be used as a suitable estimation of the optimum operating conditions for the combined continuous and preparative chromatographic system.

To investigate the optimum operating conditions by the operating principle of the system, impurity is defined as the ratio of the overlapped to unoverlapped areas of the two peaks in the desorption section. An increase in the percentage liquid loading decreases the impurity, but it increases the total elution time (Fig. 10). Because higher temperature decreases the total elution time, the impurity increases due to the fast elution of the components. It can also be seen that with higher loading of the SLP, the intersections of the two lines for one loading percentage (the solid line and the interrupted line in the figure) are shifted to higher temperature. In determining the operating conditions in the desorption section with an additional column, another significant factor is the desorbent velocity. Based on the previous results for column temperature and percentage liquid loading in Fig. 10, the effects of desorbent velocity on impurity and total elution time with the additional column lengths are shown in Fig. 11 at 35°C, 20% liquid loading, and a switching time of 240 s. In terms of additional column length (L'), the

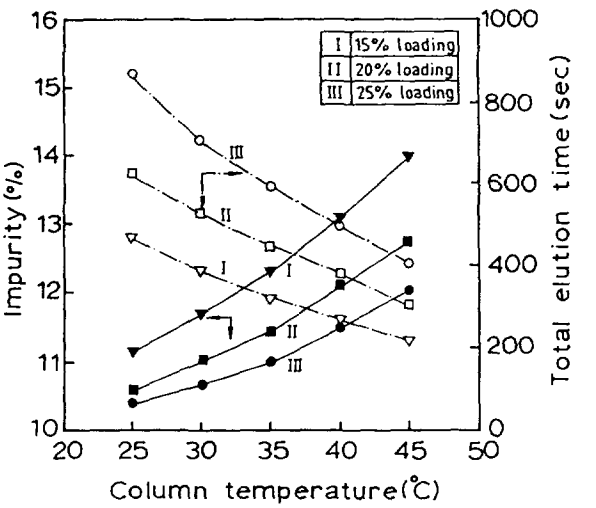

Fig. 10. Effect of column temperature on impurity and total elution time with liquid loading in desorption section. (20/30 mesh, $u_0 = 10$ cm/s, $L = 100$ cm, $L' = 50$ cm).

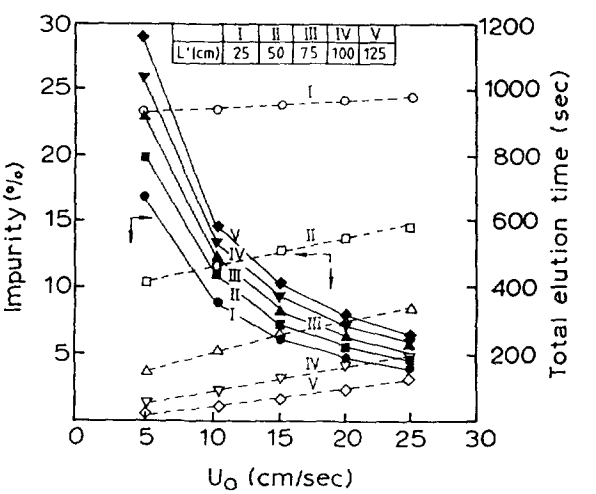

Fig. 11. Effect of desorbent velocity on impurity with additional column length in desorption section. (20/30 mesh, 35°C, $L = 100$ cm, 20% liquid loading).

solid lines show the relation between the desorbent velocity, u_0, and the total elution time, while the interrupted lines show the relation between the desorbent velocity, u_0, and the impurity. When the desorbent velocity is increased, the total elution time is increased, but the impurity is improved. When the allowable impurity is assumed to be 10%, optimum operating conditions exist for a the total elution time of less than 400 s. The optimum total elution time will be set as the switching time.

6. Conclusions

Based on the operational principle of the combined continuous and preparative chromatographic system, the experimental conditions were mainly affected by the additional column length and the desorbent velocity. The increased pressure drop caused by the longer column length and higher gas velocity could be minimized by using larger particles, and the variation of the velocity along the column was simply corrected by the average gas velocity. Because the differences between the elution profiles of the pure materials and mixtures were relatively small in this gas chromatographic system, the assumption of a linear partition relation was reasonable.

The switching time for good separation was experimentally determined, and it was mainly affected by the column temperature and column length. In spite of the small deviations caused by the assumptions of constant gas velocity and linear partition isotherm, the theoretical concentration profiles were in relatively good agreement with the experimental data. For the combined continuous and preparative chromatographic system, therefore, the uniform film thickness model can be used for the proper estimation of the optimum operating conditions.

When the feed concentration is increased, the separation mechanism in the column becomes more complex, and generally information on the nonlinear isotherms is necessary to develop the mathematical models.

Acknowledgement

The author gratefully acknowledges the financial support of INHA university in preparing this manuscript.

List of symbols

A_p	Surface area of porous particle per unit volume, cm^2/cm^3
c	Concentration of solute in mobile phase, mol/l
c_0	Inlet concentration of solute, mol/l
$C(s)$	Laplace transform of c(t)
D_e	Effective intraparticle diffusion coefficient, cm^2/s
D_l	Diffusion coefficient in stationary liquid phase, cm^2/s
D_M	Molecular diffusivity, cm^2/s
E	Effective axial dispersion coefficient, cm^2/s
k_f	Interparticle mass transfer coefficient, cm/s
k_g	Intraparticle mass transfer coefficient with respect to stationary liquid phase-film, cm/s
K	Partition coefficient
L	Column length in partition section and desorption section, cm
L'	Additional column length in desorption section, cm
n	Concentration of solute in stationary liquid phase, mol/l
q	Concentration of solute in the pore space, mol/l
r	Radial distance measured from the center of particle, cm
r_p	Radius of spherical porous particle, cm
Re	Particle Reynolds number
s	Variable of Laplace transform with respect to time
Sc	Schmidt number
SLP	Stationary liquid phase
t	Time, s
t_0	Time of feed-injection, s
T	Column temperature, K

u Interstitial mean linear velocity of carrier gas or desorbent, cm/s
u_0 Superficial velocity of carrier gas or desorbent, cm/s
u_{ave} Average velocity of carrier gas or desorbent, cm/s
x Distance perpendicular to surface of porous particle, cm
z Axial distance, cm

Greek letters

$\gamma, \gamma_1, \gamma_2, \gamma_3, \gamma_4, \gamma_5$ Values defined by Eqs. 22–27
δ Film thickness of stationary liquid phase, μm
ϵ Interparticle void fraction of chromatographic column
ϵ_p Intraparticle void fraction with presence of stationary liquid phase
$\lambda, \lambda_1, \lambda_2, \lambda_3$ Values defined by Eq. 12–15

References

[1] A.T. James and A.J.P. Martin, Analyst, 77 (1952) 915.
[2] Eli Grushka (Editor), Preparative-Scale Chromatography, Marcel Dekker, New York and Basel, 1989.
[3] G. Subramanian, Preparative and Process-Scale Liquid Chromatography, Ellis Horwood, New York, 1991.
[4] R.G. Bonmati, G. Chapelet-Letourneux and J.R. Margulis, Chem. Eng., 87 (1989) 70.
[5] P.E. Barker, in C.H. Knapman (Editor), Developments in Chromatography, Applied Science Publisher, London, 1978.
[6] D.B. Broughton, Chem. Eng. Pro., 64 (1969) 60.
[7] P.C. Wankat, Ind. Eng. Chem. Fundamen., 16 (1977) 468.
[8] H.Y. Ha, K.H. Row and W.K. Lee, Sep. Sci. Technol., 22 (1987) 141.
[9] H.Y. Ha, K.H. Row and W.K. Lee, Sep. Sci. Technol., 22 (1987) 1281.
[10] P.C. Wankat, Ind. Eng. Chem. Fundam., 23 (1984) 256.
[11] K. Hashimoto, S. Adachi, H. Noujima and A. Maruyama, J. Chem. Eng. Jpn., 16 (1983) 400.
[12] K. Hashimoto, S. Adachi, H. Noujima and Y. Udea, Biotechnol. Bioeng., 25 (1983) 2371.
[13] P.E. Barker and R.E. Deeble, Anal. Chem., 45 (1973) 1121.
[14] P.E. Barker, F.J. Ellison and B.W. Hatt, Ind. Eng. Chem. Process Des. Dev., 17 (1978) 302.
[15] P.E. Barker and C.H. Chuah, Chemical Engineer, Aug./Sept. (1981) 389.
[16] P.E. Barker, K. England and G. Vlachogiannis, Chem. Eng. Res. Des., 61 (1983) 241.
[17] C.B. Ching and D.M. Ruthven, Chem. Eng. Sci., 40 (1985) 877.
[18] C.B. Ching and D.M. Ruthven, Chem. Eng. Sci., 40 (1985) 1411.
[19] K.H. Row and W.K. Lee, Sep. Sci. Technol., 22 (1987) 1761.
[20] K.H. Row and W.K. Lee, J. Chem. Eng. Jpn., 19 (1986) 173.
[21] M.A. Alkarasani and B.J. McCoy, Chem. Eng. J., 23 (1982) 81.
[22] N.D.P. Dang and L.G. Gibilaro, Chem. Eng. J., 8 (1974) 157.
[23] I. Moon, K.H. Row and W.K. Lee, Korean J. Chem. Eng., 2 (1985) 155.
[24] H.M. McNair and A.J.P. Bonelli, Basic Gas Chromatography, Varian Aerograph, Berkeley, CA, 1969.
[25] K.H. Row and W.K. Lee, in N.P. Cheremisinoff (Editor), Separation by Gas–Liquid Chromatography, Handbook of Heat and Mass Transfer, Vol. 3: Catalysis, Kinetics, and Reactor Engineering, Ch. 22, Gulf Publishing Company, Houston, TX, 1989.
[26] A. Littlewood, Gas Chromatography, Academic Press, New York, 1970.